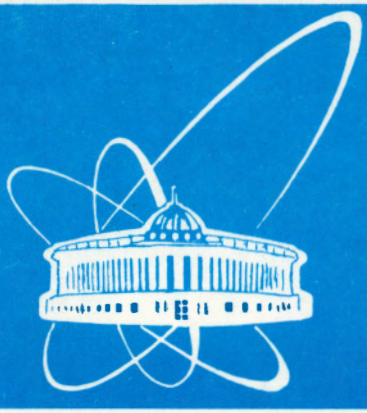

объединенный
институт
ядерных
исследований
дубна

E7-94-245

Yu.Ts.Oganessian, Yu.E.Penionzhkevich

JINR HEAVY ION PROGRAM OF LOW AND MEDIUM ENERGIES

Invited talk at the International Conference on Mesons and Nuclei at Intermediate Energies, Dubna, May 3—7, 1994

1994

Heavy ion beams have opened wide prospects for investigating the properties of nuclear matter in its extreme state - at high values of the isotopic spin, deformation, angular moment and excitation energies. Such exotic states of nuclei are being studied at the Flerov Laboratory of Nuclear Reactions with the use of beams of heavy ions in the 5 MeV/A≤E≤100 MeV/A range. The Laboratory has three heavy ion cyclotrons - U-200, U-400 and U-400M. Their characteristics are given in Table I. The high beam intensity , up to 2-4×10 ^{13} pps, is worth noting. It allows investigating processes with a cross-section approaching 10^{-35} cm^2. The FLNR accelerator facilities are constantly being developed. A tandem combining the U400 and U400M cyclotrons has been designed, extending the range of accelerated particles up to uranium and increasing the energy of the heavy Xe-U nuclei.

Table I.

Characteristics of the FLNR heavy-ion accelerator facilities

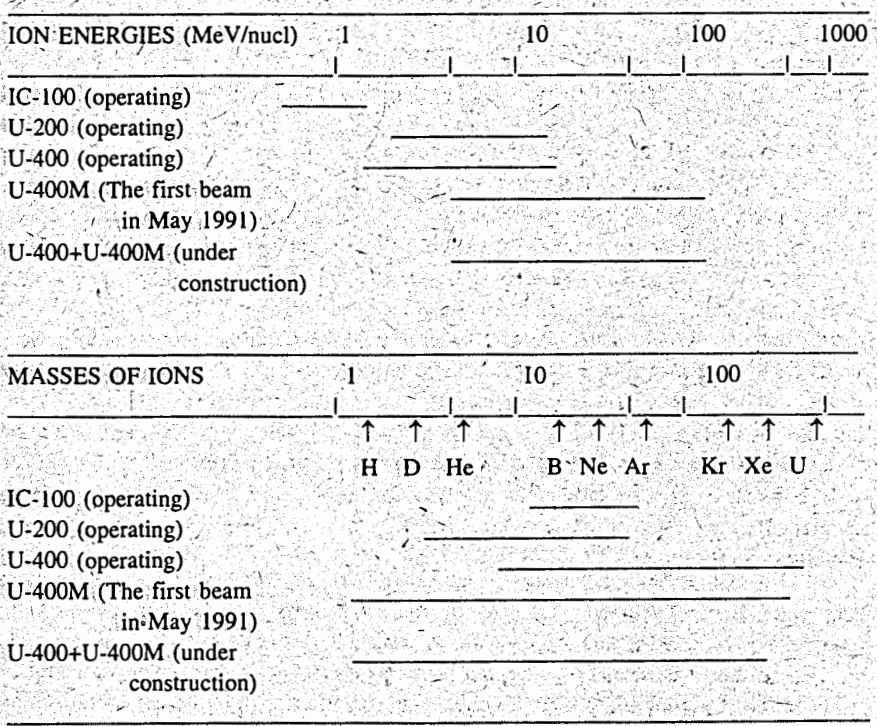

The U-400 cyclotron has been in operation over 10 years. It has been used for research in fields traditional for FLNR involving low energy physics(E≤20 MeV). Primarily, these are fusion reactions producing new trans-fermium elements. The stability of trans-fermium elements and their properties are entirely determined by shell corrections to the liquid drop barrier [1]. The stabilising role of the shell effects manifests itself at excitation energies E≤40 MeV not only in the ground state but also in the deformed state of the nuclei. The theory considering the shell corrections (they are just a few MeV while the total energy of the nuclei is several GeV) provides sufficient explanation for most experimental facts, i.e. rising of the fission barriers and isomerism of actinide nuclei, spontaneous fission of trans-actinides, changes in the $T_{s.f.}$ near the shells, in particular with N=152, etc. These effects cannot be explained from the standpoint of the classical liquid drop model. That is why the so called cold-fusion reactions are effectively used for the synthesis of new nuclei. In these reactions targets and projectiles close to the magic nuclei (e.g. ^{208}Pb and ^{48}Ca) are used. The minimum excitation energy of the compound nuclei, determined by the Coulomb barrier and by the difference between the nuclear masses, then amounts to only E^*_x =18-20 MeV [2]. The transition of such nuclei into the ground state is accompanied by emission of one or two neutrons and γ-quanta. The majority of isotopes of elements with Z≥104 have been synthesised in cold fusion reactions. However, any further advance into the Z≥110-114 region by means of cold fusion poses the problem of using a heavy bombarding particle with A≥50, which in its turn leads to limiting the probability of fusion due to the strong Coulomb forces (Z_1Z_2≥2000) [3]. For example, the cross-section of the ^{208}Pb (^{62}Ni,n)^{270}110 reaction producing element 110 was 1 pb (10^{-36}cm^2) [4]. Therefore, for the synthesis of nuclei with Z≥108 are used very asymmetrical target-projectile combinations (Z_1Z_2≈1000) for which dynamic limitations of the fusion are not very significant. Meanwhile, the minimum excitation energy for hot fusion reactions is E^*_{min}≈40 MeV. At such excitation energies the fission barrier is determined mainly by the macroscopic component (liquid drop) of the nucleus deformation energy, which is practically zero for trans-actinide nuclei (Fig.1). Such nuclei decay into the ground state emitting a neutron cascade (x≥4) and the probability of residual nucleus (EVR) formation will be determined to a large degree by the dynamic properties of the excited compound nuclei, which may depend on different parameters of the nucleus. Thus, it was demonstrated that the drop in the cross-section of EVR formation for superheavy elements (Z≥106-108) in hot fusion reactions is not as dramatic as predicted by conventional models considering only one-particle excitations in nuclei (Fig. 2).

Hence, the Flerov Laboratory of Nuclear Reactions carries out experiments involving the synthesis of trans-actinide nuclei in cold and hot fusion reactions. Two separators are used in these experiments - a gas-filled separator [5] and the kinematic separator 'VASILISA' [6] combining electric and magnetic fields. Both separators utilise the

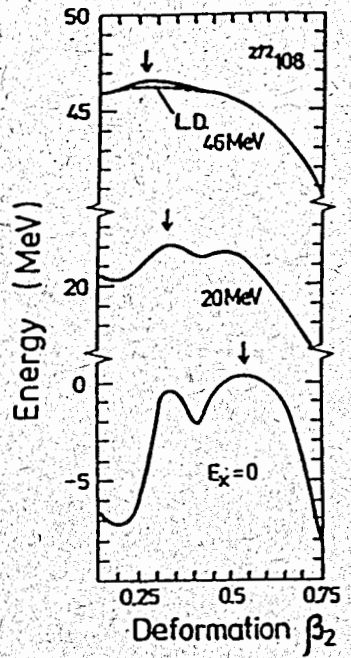

Fig. 1. Energy of the ^{272}108 nucleus vs. its deformation at different excitation energies indicated in the figure (LD - liquid drop component E_{LD}).

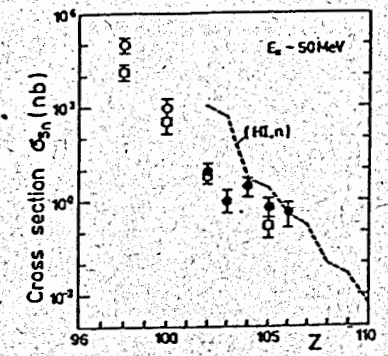

Fig. 2. The cross-sections σ_{5n} (○,●) and σ_{6n} (□) vs. the atomic number of EVRs. Nuclei of Cf and Fm were produced in ^{16}O-induced fusion reactions and nuclei with Z=102-106 in reactions induced by ^{22}Ne, ^{26}Mg, ^{27}Al. The dashed line is drawn through the experimental cross-section values of (HI,n) - cold fusion reactions.

difference between the angular distributions of the recoil nuclei in complete and incomplete fusion for separating the products of the two processes. Since both separators are positioned at 0° relative to the primary beam it is necessary to separate the recoil nuclei from those of the beam.

In the gas-filled separator at low gas pressure (H or He) the charge of the recoil nuclei changes depending on their velocity. This allows, in the magnetic field, highly efficient separation of the recoil nuclei of complete fusion reactions from others (those of incomplete fusion, the beam nuclei and nuclear scattering). From the characteristics of the gas-filled separator presented in Table II follows that the purification coefficient may reach several units of 10^{16}. In 1993-1994 a series of experiments using this separator and a system of position-sensitive silicon detectors was carried out in collaboration with the LLNL (Livermore) to investigate the stability of neutron-rich isotopes of element 106 in the ^{248}Cm + ^{22}Ne reaction [7]. At ^{22}Ne energies of 116 MeV and 121 MeV corresponding to the maximum of the excitation functions of the complete fusion reactions emitting 4 and 5 neutrons two new isotopes ^{266}106 and ^{256}106 were synthesised. Fig. 3. presents the theoretical and experimental lifetimes of element 106 isotopes relative to spontaneous fission and α-decay. It is seen that in the

Table II

Characteristics of the Dubna gas-filled recoil separator.

Target	^{nat}W	$^{235,238}U$	^{235}U	^{242}Pu	^{238}U	$^{206,207}Pb$	^{207}Pb
Projectile	^{22}Ne	^{18}O	^{22}Ne	^{22}Ne	^{26}Mg	^{34}S	^{40}Ar
Z of EVRs	Po	Fm	102	104	104	Cf	Fm
Beam energy (MeV)							
$<E_R>$ (MeV)	112	93	122	114	134	170	196
$<q>$	11.0	5.8	8.7	7.0	11.5	21.8	28.2
ε_c (%)	3.3±0.1	2.1±0.1	2.3±0.1			4.8±0.2	5.9±0.2
	16±3	3±1	6±2	6±2	10	35±10	45±10
Suppression of full energy projectiles	$>10^{15}$	$>5\times10^{16}$	$>10^{17}$	$>2\times10^{18}$	$>4\times10^{17}$	$>3\times10^{15}$	
scattered projectiles with E>35 MeV			2×10^{16}	7×10^{16}	5×10^{15}	10^{14}	5×10^{12}
target-like products	$>10^3$			$>10^4$			5×10^4
Image size (full width at half-maximum)							
horizontal	6.8±0.2	8.7±1.4	12.3±3			7±1	
vertical	2.1±0.1	3.5±0.2					

region of the deformed shell N=162, the lifetime is significantly longer than its theoretical predictions ($T_{s.f.}$ (^{266}106)=1,$3^{+1,6}_{-0,8}$ s). This provides evidence of the existence of a high stability region for superheavy elements. At present experiments are being carried out with the gas-filled separator to study the stability of neutron-rich isotopes of element 108. These experiments will ultimately resolve the controversial issue of the existence of the stability region for superheavy elements.

Experiments with the 'VASILISA' spectrometer are being carried out to investigate the mechanism of hot fusion producing compound nuclei at excitation energies of up to 200 MeV. Fig. 4 presents a typical excitation function for a fusion reaction involving the emission of x neutrons (x=3-12).

It can be seen that for the fissioning nuclei the probability of survival of the compound nuclei with high excitation energy is relatively high. Of great interest are direct measurements of the cross-section of compound nuclei formation at beam energies of up to 40 MeV/A (E^*≈400 MeV). Such measurements are expected to be performed on the U-400M cyclotron in the $^{186}W(^7Li,xn)Ir^{175-169}$ reaction (where x=18-24). In this reaction compound Ir nuclei will be measured by means of registering their α-decay. The experiment is expected to be performed in collaboration with Lanzhou Institute of Physics (China).

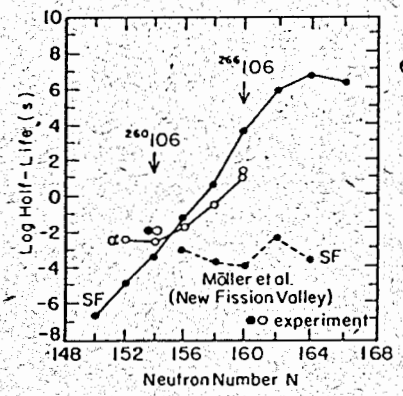

Fig. 3. The half-lives of isotopes of element 106: ○,● - α decay and spontaneous fission half-life (seconds), the full line is drawn through the calculated values of T_α and $T_{s.f.}$ [8,9]. The dashed line connects the $T_{s.f.}$ values calculated in the symmetric fission valley [10].

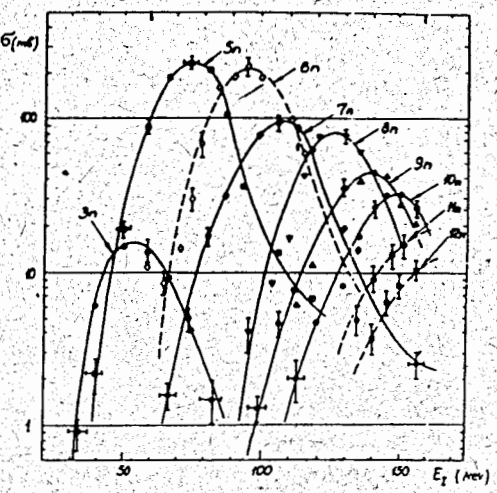

Fig. 4. Excitation functions for the reaction $^{130}Te(^{13}C,xn)^{143-xn}Ce$.

Simultaneously with further increase of the energy of the bombarding particle the cross-section of the reactions producing compound nuclei begins to decrease dramatically due to the competitive emission of pre-equilibrium charged particles. This process takes place even at energies close to the Coulomb barrier [11]. At energies of 10 MeV/A the cross-section of pre-equilibrium α-particle emission comprises a significant part of the total reaction cross-section. With the use of a magnetic spectrometer having high momentum resolution and multi-layer scintillating detectors, systematic investigation of energy spectra of light charged particles has been performed at FLNR in a wide range of energies up to the maximum available for a given reaction and determined by the energy conservation laws supposing a two-body nature of the mechanism for the production of fast particles (breakup-fusion).

Fig. 5 displays the energy spectra for light particles produced in the ^{181}Ta +^{22}Ne reaction. The arrows in the diagram indicate the value of the two-body kinematic limit corresponding to the fusion of the projectile residue (I-LP) and the target and producing a final nucleus in the ground state. Application of a multi-layer scintillation telescope improved the sensitivity of such experiments. Fig. 6 presents the energy spectrum of protons measured with the aid of the telescope. It shows that at bombarding beam energies of 20 MeV/A, protons with energies up to 160 MeV are observed in the spectrum.

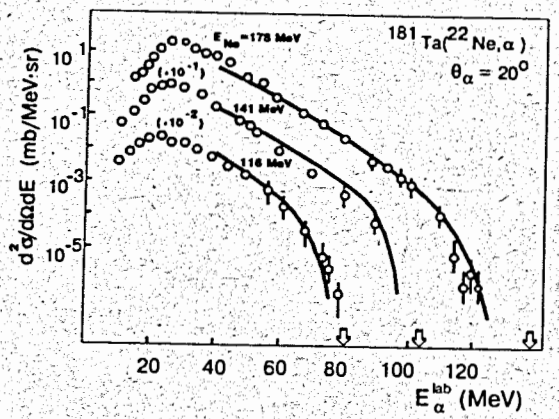

Fig. 5. Inclusive energy spectra of α-particles from the reaction $^{181}Ta(^{22}Ne,\alpha)$ measured at θ_α =20° for the beam energies 116, 141 and 178 MeV. The arrows indicate the maximum possible energies assuming a two-body reaction mechanism [12]. The solid lines represent the result of theoretical calculations within the dissipative massive transfer model [13].

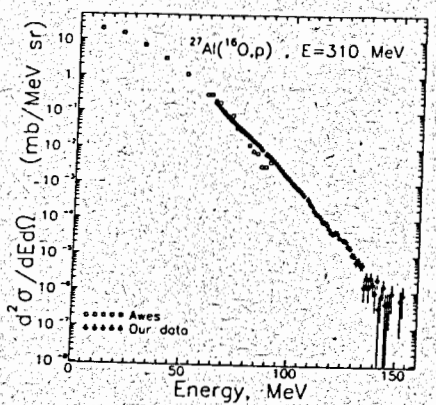

Fig. 6. Energy spectrum of protons produced in the reaction $^{27}Al(^{16}O,p)$ at E=310 MeV [14].

The following conclusions about the properties of energy spectra of light charged particles were made:

An increased yield for α-particle emission was observed in comparison to other particles, even to protons. The maximum of the energy spectrum is lying at light particle velocities less than the beam velocity, which provides evidence for a significant role of the relaxation processes at the stage of light particle emission. With an increase in the beam energy the peak of the double differential emission cross-section of light particles shifts in the direction of the energies corresponding to the beam velocity. However, even at energies a few tens of MeV/A in the spectrum of forward- peaked light particles there is a considerable dissipative contribution (V_c^b (α)< E_α<E_α^{beam}).At a smaller projectile mass A_1 the peak in the spectrum approaches V_{beam} which implies a decrease in the 'dissipative' part of the spectrum. With an increase in the projectile energy the maximum value of the differential cross-section $\frac{d^2\delta}{d\Omega dE}$ (V_{LP}^{opt}) at first rapidly rises(by a factor of ten at the transition from E_1=5 MeV/A to E_1=20 MeV/A), and then a saturation is observed. And finally, for low energies ~ 10 MeV/A the energy spectrum of light particles extends up to the two-body kinematic limit, corresponding to the fusion of the projectile residue (I-LP) and the target accompanied by the production of a final nucleus in the ground state, an abrupt change

being observed at the very end of the spectrum. The analysis of these data as well as the results of other experiments show that the energy spectra of light charged particles reflect all possible interaction mechanisms between ions and nuclei at low and medium energies. In ref.[15] are pointed out 4 basic mechanisms for light particle production

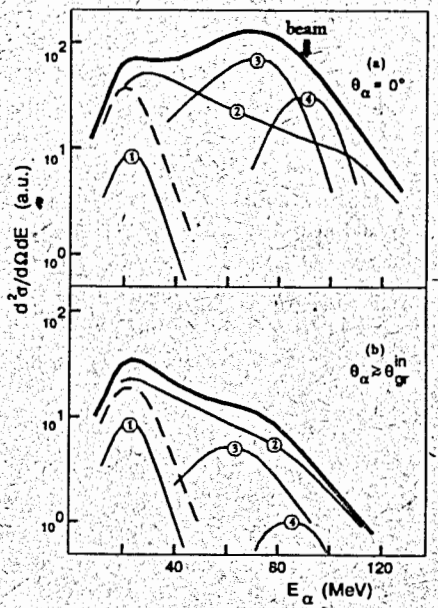

Fig. 7. Schematic picture of the α-particle energy spectra and of expected contributions of the four mechanisms of their formation at beam energies ~20 MeV/A: (1) - evaporation from the compound nucleus, (2) - incomplete fusion reaction, (3) - inelastic breakup, (4) - elastic breakup. The dashed line corresponds to the total yield of evaporative α-particles (from process (1) and from any other heavy residues formed in processes (2) and (3)).

1. The process of complete fusion of the nuclei with subsequent evaporation of light particles from the compound nucleus or from fission fragments. A distinctive feature of the evaporating particles is their low energy and isotropic angular distribution.

2. The initial two-body process of incomplete fusion with emission of only one pre-equilibrium particle . The light particles produced in this process can be fast (up to energies corresponding to the two-body kinematic limit E_{RP}^{max}) or slow. They can be formed both from the projectile nucleons (massive transfer) and the target nucleons (knock-on process). These particles cannot be accompanied by other particles, however, they may be accompanied by slow (evaporation) light particles, neutrons or fission fragments.

3. The two-body primary process of few-nucleon transfer inelastic excitation (ΔA=0) followed by decay of the excited projectile-like nucleus. This process produces both fast and slow light particles. The former are accompanied by fast projectile-like fragments or other fast particles, the latter (when the dissipation is high) are accompanied only by slow fragments. This group of the mechanisms should also include the deep-inelastic excitation of the target and the projectile either without any mass transfer (ΔA=0) or with mutual exchange of an equal number of nucleons.

4. The quasi-inelastic break-up process of the incident ion and the quasi-inelastic process of knocking out a light particle from the target. It is rather difficult to experimentally discriminate between these processes , because the evaluation of the total cross-section of a three-body process requires integration over all the angles of the complementary fragment which can be performed only by means of a 4-π detector.

Naturally, this differentiation of the processes is purely conventional. Besides, it depends on the mass and energy of the incident ion. However, it points to the possibilities for investigating the light particle emission mechanism. This investigation should be performed with the aid of detectors allowing high-sensitivity measurement (geometrical efficiency, capability to use high intensity initial beam) of the energy spectra and cross-sections, as well as granularity and geometry close to 4π making it possible to measure the correlations, the multiplicity and angular distributions. FLNR has two facilities with these features - the 4π detector of multiple events FOBOS [16] and the system of multilayer scintillation telescopes in conjunction with the BGO-ball from LAMPF (Los Alamos) [17] to be installed at the beam of the U-400M cyclotron.

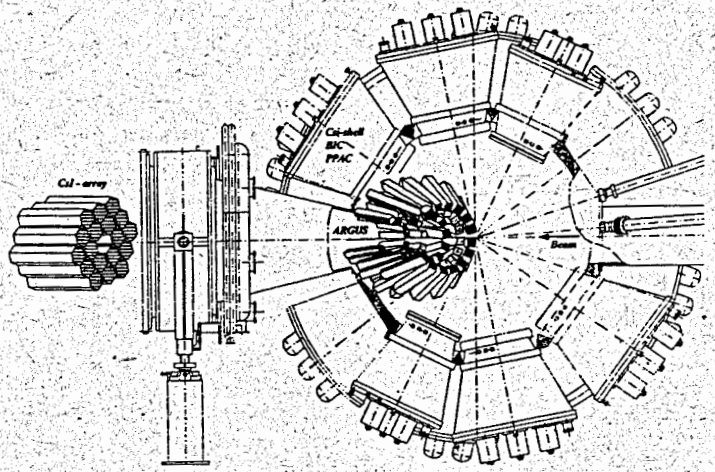

Fig. 8. The FOBOS set-up.

Fig. 8 presents a general view of the FOBOS facility and Table III displays its characteristics. The facility has 30 gas-filled detectors which are parallel-plate avalanche counters, providing a time-signal and measuring the incidence co-ordinates of the particles. These are followed by Bragg-ionisation chambers measuring the energy and the charge of the particles and fragments. And finally there are scintillation Cs(I) detectors allowing identification of fast particles by means of pulse shape and measurement of their energy. The BaF_2 scintillation multidetector ARGUS from HMI (Berlin) is proposed as the forward detector. This facility is under construction within the Dubna - Rossendorf - Berlin -Krakow - Sofia collaboration. Research in the following directions will be conducted with its aid:

Table III.
Characteristics of the FOBOS facility.

Particle	PPAC + BIC		CsI Shell *[15mm]*		ARGUS array *BGO [20mm]*		Array "O-deg." *CsI [150mm]*	
	E min MeV/A	E max MeV/A	E min MeV/A	E max MeV/A	E min MeV/A	E max MeV/A	E min MeV/A	E max MeV/A
H	---	---	1.5	63.0	2.0	100.0	5.0	250.0
He	0.2	4.0	2.0	65.0	2.0	101.0	5.0	253.0
Li	0.2	5.0	2.0	82.0	3.0	125.0	7.0	320.0
IMF (Z<15)	0.15	10.0	----	----	4.0	150.0	----	----
FF	0.15	10.0	----	----	----	----	----	----

1. Investigation of the induced binary, ternary and multiple fission of heavy nuclei in reactions with ions from ^{7}Li to ^{40}Ar at energies E_I<30 MeV/A, including light nuclei fission with emission of two clusters ($^{28}Si \rightarrow {}^{16}O+{}^{12}C$, $^{24}Mg \rightarrow {}^{12}C+{}^{12}C$) [18].

2. Investigation of the emission mechanism for fast charged particles in coincidence with residual nuclei decay products at $E_I \leq 30$ MeV/A. In that case the charged particle may act as a trigger for the selection of a defined state of the residual nucleus according to its excitation energy and angular momentum.

3. Investigation of the target nucleus fragmentation and measurement of the particle multiplicities and their correlations, including those for backward angles. These experiments can provide an explanation for the characteristics of the transformation processes with complete momentum transfer and complete fragmentation . New mechanisms are expected to be revealed here, including the semiperipheral mechanism of deep-inelastic transfer with the formation of intermediate mass fragments from the neck region at the energy of $E_I \approx 40$ MeV/A, predicted by M. Di Toro [19].

4. Investigation of the multifragmentation process near the E_I = 40 MeV/A threshold.

5. Reactions with radioactive beams. The problem of obtaining beams of radioactive nuclei will be considered later in this paper.

Important information on the mechanism of heavy ion reactions can be obtained while investigating emission of high energy γ-quanta with $E_\gamma > E_I/A_I$. Investigation of the electromagnetic radiation characteristics for this purpose is in some cases more informative than investigation of light charged particle emission [20]. Firstly, the relative weakness of electromagnetic interaction allows application of lower orders of the perturbation theory. Secondly, the structure of electromagnetic currents is well known and this eliminates any uncertainty in constructing the matrix elements of the emission process. Thirdly, there is no problem of the nuclear field affecting the

emitted particle - a photon. And finally, the relatively small momentum of the photon in some cases allows utilizing the multipole expansion of the amplitude of the electromagnetic interaction.

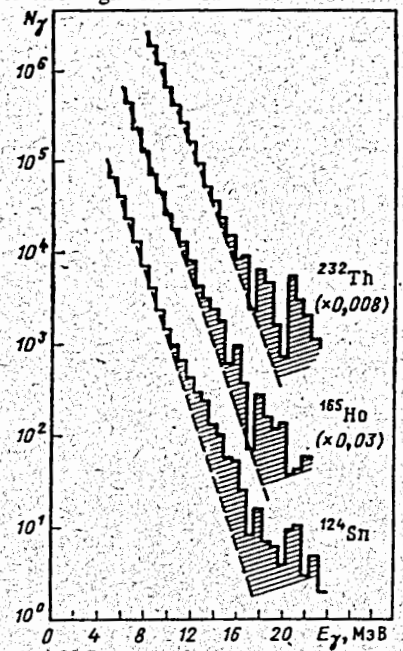

Fig. 9. Spectra of γ-rays measured by ^{22}Ne-induced reactions on different targets.

Studies of the rigid component of γ-radiation in reactions with heavy ions at energies up to 20 MeV/nucleon have been performed at FLNR [20]. Various combinations of scintillation NaI, CsI and BGO detectors were used. The discovery of the complex nature of the γ-ray emission with $8<E_\gamma<30$ MeV was one of the main results. It provided experimental evidence of an increase in γ-ray emission in comparison with the calculated values from the formula $Y_\gamma \sim \exp(-E_\gamma/T)$ for $E_\gamma>8$ MeV (Fig. 9). The bumps observed in the experimental γ-quanta spectra for $E_\gamma>8$ MeV was interpreted as excitation of the giant dipole resonance (GDR) in the compound nuclei. The shapes of high-energy γ-quanta were measured depending on the parameters of the compound nuclei. A double-peak spectral shape corresponding to GDR fission due to the large angular momentum of the compound nuclei was revealed. Angular anisotropy of high-energy γ-quanta has been studied. A special feature of these experiments was selection of the formation channel of residue nuclear products by a direct technique according to the registered characteristic x-ray emission, fission fragments or light charged particles [21].

The main results of the measurements could be stated as follows:

1. The emission of γ-quanta can be explained by three processes - statistical, bremsstrahlung and that involving excitation with subsequent multipole giant resonance decay. At $E_\gamma<30$ MeV all three processes contribute significantly, at $E_\gamma>30$ MeV the bremsstrahlung radiation has the greatest contribution. For discriminating between the contributions of these processes it is necessary to select the reaction channel during the measurements.

2. High-energy photon emission ($E_\gamma>30$ MeV) evidently takes pace at an early stage of the collision process.

3. In the E_γ = 30 MeV range γ-spectra shape irregularities ('bumps') cannot be explained within statistical approaches. One can suppose that the 'bumps' are linked to the decay of collective nuclear states.

4. A comparison of the obtained experimental data on the energy and angular γ-quanta distribution with the available information on the sub-threshold production of π-mesons in analogous reactions allowed a supposition about possible similarity of the production mechanisms of high-energy γ-quanta and π-mesons.

This supposition allows a different view of the formation mechanism of the sub-threshold pion production in reactions with medium-energy heavy ions. Just as in the case of high-energy γ-quanta, in reactions with heavy ions at the energy of E_l/A_l=25 MeV/A in the independent particles model one- or two-nucleon pion production mechanisms are either kinematically forbidden or have a negligible low probability (e.g. taking into account the internal movement in colliding nuclei). Then arises the question about the physical mechanism of conveying a considerable portion of the collision energy to the π-meson, which is absent from the mass surface of the system. Compared to an analogous process of the high-energy photon production, obtaining experimental information about π-meson characteristics is more difficult due to a relatively low probability of its production (the cross-section range is from one to several nanobarn (Fig. 10). Besides, investigation of neutral and charged pion spectra correspondingly requires different techniques, which makes a direct comparison of the obtained results difficult (e.g. there are practically no experimental results on the angular distribution of π-mesons). Identification of π^0-mesons is done by means of measuring the coincidence of the two high-energy γ-quanta from the $\pi^0 \rightarrow \gamma+\gamma$ decay, occurring with 98.8% probability. The characteristics of charged mesons are determined either by a scintillation telescope or by a magnetic spectrometer. Measurements of neutral pions have advantages over charged π-meson measurements [22].

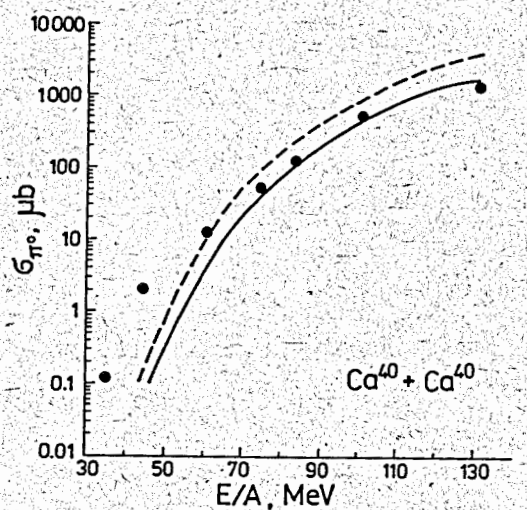

Fig. 10. Excitation function for π° productions in the reactions $^{40}Ca + ^{40}Ca$.

1. γ-quanta registration can be done in a comparatively large solid angle (5-10% of 4π), which allows measuring cross-section of about 10^{-33}cm².

2. The Coulomb field of the daughter nucleus does not distort the measured spectral and angular characteristics of π^0-mesons.

3. For registration of π^0-mesons there is no low energy threshold. One can measure π^0-meson productions with energies practically equal to zero.

A joint Dubna - Los-Alamos - Rez experiment at the U-400M accelerator in FLNR JINR is planned for systematic investigation of the mechanisms of high-energy γ-quantum and π^0-meson formation at the energy of $E_l \sim 50$ MeV/A. Multilayer scintillation and semiconductor telescopes, the 4-π BGO ball from LAMPF [17] and the BGO-wall from IPN (Rez, Czech Republic) will be used for this purpose. Fig. 11 presents a schematic view of the experimental set-up. Table IV displays the characteristics of the BGO-ball and the scintillation detectors.

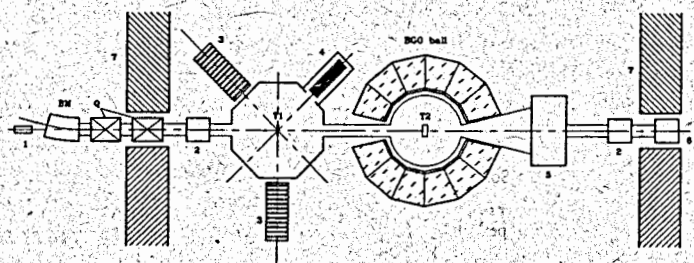

1 – laser for setup alignment
BM – bending magnet
Q – quadrupoles
2 – pump and beam diagnostic box
3 – scintillation telescope
4 – semiconductor detector telescope
5 – forward detector
T1,T2 – targets
6 – Faradey cup
7 – concrete shield

Fig. 11. A schematic view of the experimental set-up to be used for studies of the mechanism of high-energy γ-quanta and π°-meson production.

The following programme of experiments is planned:

1. Measuring the angular distribution of the emitted π^0-mesons, including those at backward angles. This will allow determining respective contributions of the coherent and the incoherent sources of pion emission.

2. Investigation of the spectral distribution with simultaneous registration of the pion and scattered ion emission angles. Possible diffraction structure of such distribution

Table IV.
Characteristics of the BGO-ball and scintillation detectors.

4π-BGO detector parameters

A number of plastic-BGO phosvich-detectors	30
Solid angle	0.88•4π *sr*
Thickness of plastic scintillator	3 *mm*
Thickness of BGO-crystall	5.6 *sm*
Maximal detect proton energy	185 *MeV*
Maximal detect pion energy	90 *MeV*

Characteristics of semiconductor and scintillation detectors

	SCD-telescope	*Scint.telescope*
Proton energy range	6-50 *MeV*	20-230 *MeV*
Pion energy range	3-25 *MeV*	10-100 *MeV*
Energy resolution	0.5-0.7 *MeV*	2-3 *MeV*
Solid angle	1-20 *msr*	1-30 *msr*
Max. number of events per second	10^5 *sec*$^{-1}$	10^6 *sec*$^{-1}$

could be an indication of the 'nuclear bremsstrahlung' mechanism of the π^0-meson emission and provide precision data about the form of the inter nuclear potential.

3. Investigation of the energy and mass dependence of the threshold in pion emission. This would also assist a more concrete definition of the reaction mechanism.

4. Investigation of pion spectra on the high-energy side in the kinetic energy range above 200 MeV. Detection of a relative enhancement in the π^0-meson yield alongside their energy increase will provide a more precise understanding of the role played by the Δ-resonance mechanism of pion production.

And, finally, one of the topical tasks pursued at many heavy ion research centres of the world is investigation with radioactive beams. FLNR also has a programme in this field. With the advent of radioactive nuclei beams it has become possible not only to study their properties, but also to study reactions induced by them. The main problem of producing secondary beams is linked with the synthesis of radioactive nuclei. At present, direct reactions producing radioactive nuclei at energies up to 20 MeV/A and projectile fragmentation reactions at energies of $E_n \geq 50$ are the most effective ones. In the first case neutron and proton stripping and pickup reactions are used, as well as

transfer reactions and (p,2p), (p, 3p) and (p, He^3) reactions on hydrogen targets using inverse kinematics. In these reactions the energy resolution of the secondary beam can be 1-3%. Using the maximum intensity of low energy ions (10^{13}-10^{14}1/s), beams of ^{6}He,^{9}Li, ^{12}Be, etc. can be produced with intensities up to 10^6 1/s. Radioactive beams of secondary low energy particles are of great interest in investigating nuclear reactions induced by them close to the Coulomb barrier. A few years ago it was demonstrated that in the very neutron-rich nuclei of light elements, such as ^{11}Li, ^{14}Be and others, there can be neutron halos characterised by a large root-mean-square radius of the neutron distribution [23] (Fig. 12). Thus, for the ^{11}Li nucleus this radius proved to be close to the neutron distribution radius of the uranium nucleus (~13 fm). This allowed a number of predictions to be made about the peculiarities of interactions of such nuclei - a relatively high cross-section of the sub-barrier nuclear fusion of halo nuclei producing weakly-excited compound nuclei, sub-barrier valence neutron transfer and excitation of the soft mode of giant resonances. At the U-400M cyclotron in FLNR radioactive beams of ^{6}He, ^{9}Li and ^{11}-^{12}Be have been produced with energies of ~10 MeV/A. They have been used to investigate elastic scattering and fusion-fission reactions. Fig. 13 displays the ratio between the elastic scattering cross-section of ^{6}He, ^{6}Li, ^{9}Li and Rutherford scattering versusthe parameter of closest approach between two nuclei in the quasi-classical approach [24]. It is seen that the curves for ^{6}He and ^{6}Li coincide, which corresponds to the same interaction radii between these nuclei and ^{208}Pb nuclei and diffuseness. The curve for ^{9}Li is different and has a large interaction radius, which permits the conclusion about a high degree of deformation of this nucleus, which is close to the nucleus having a neutron halo (^{11}Li), in the Coulomb field of the target-nucleus. With the use of the secondary ^{6}He beam the excitation function of the fusion-fission reaction ^{6}He +^{209}Bi in the $E_{C.M.}$= 30-50 MeV was studied [25] (Fig. 14). A comparison of the cross-section data for ^{209}Bi fission by ^{4}He and ^{6}He nuclei shows that at the same excitation energy the cross-section of ^{209}Bi fission by ^{6}He nuclei is

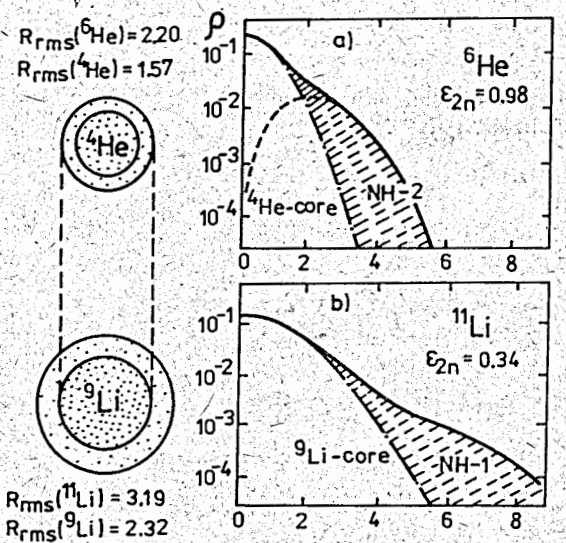

Fig. 12. A presentation of the neutron density distributions for ^{6}He and ^{11}Li, showing the difference between two types of halo (1st type - ^{11}Li, 2nd type - ^{6}He).

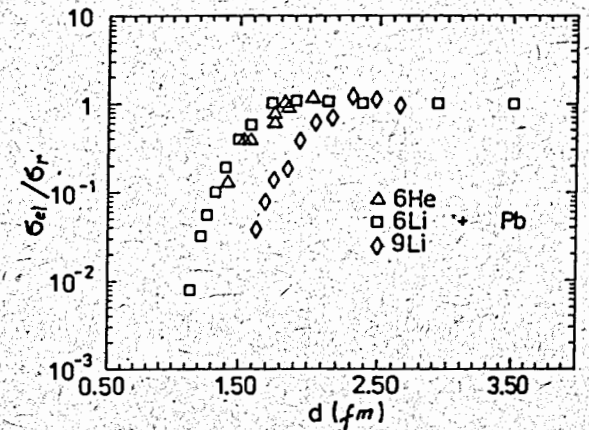

Fig. 13. σ_{el}/σ_r vs. the parameter of the distance of closest approach [24].

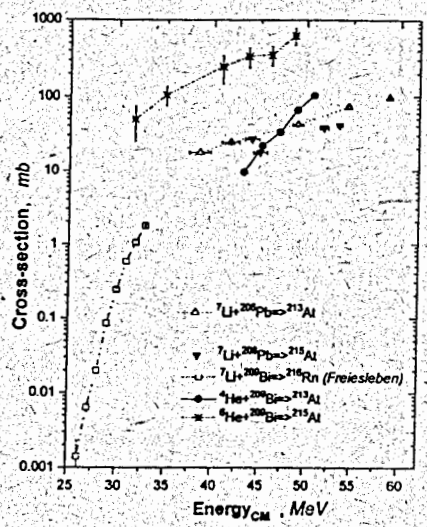

Fig. 14. Excitation function for the fusion-fission reaction ^{6}He + ^{209}Bi for $E_{c.m.}$=30-50 MeV. Other reaction cross sections are shown for comparison.

about 5 times larger than that for ^{4}He nuclei. A large energy shift between the thresholds of these reactions also attracts attention. It is indicative of an increase of the Coulomb barrier of the fusion for the nuclei having the neutron halo (^{6}He). Unfortunately, the restrictions imposed by the target thickness in the case of using low-energy primary beams do not allow a large yield of secondary nuclei, particularly in the mass range of A≥10. Fragmentation reactions are used for such radioactive beams at primary ion beam energies of E_i=50-100 MeV/A. For producing a secondary beam of exotic nuclei it is necessary to use beams of highly-neutron-rich or neutron-rich nuclei, such as ^{36}Ar, ^{36}S, ^{48}Ca and others. Joint Dubna-GANIL (France) experiments with the use of ^{48}Ca beams have demonstrated its advantages for producing highly-neutron-rich nuclei in fragmentation reactions. Fig. 15 displays

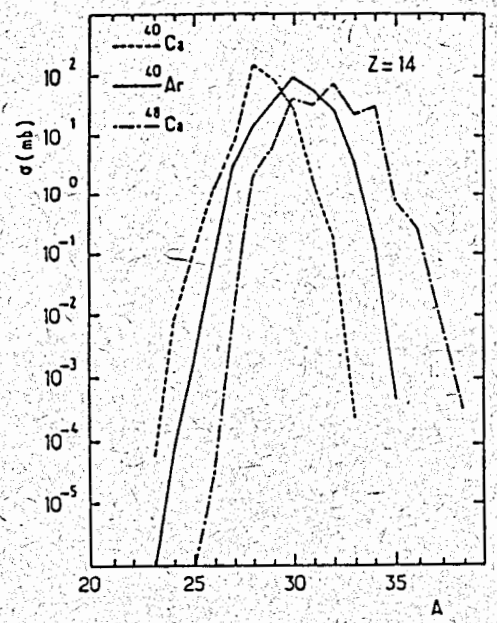

Fig. 15. Calculated final distributions for t=14 isotopes produced with three different projectiles including ^{40}Ca and ^{48}Ca (E_{inc}=44 MeV/A, Ta target) (taken from ref. 26).

isotopic distributions of Mg in the case of ^{48}Ca and ^{40}Ca fragmentation. In these experiments about 40 nuclei on the nucleon stability border have been synthesised for the first time [27]. It should be noted, that in reactions with ^{48}Ca ions at the energy of ~60 MeV/A nuclei with the mass of A≥48 were also observed. It is indicative of the fact that at such energies besides the fragmentation of the projectile nucleus, reactions similar to deep-inelastic transfer reactions can also occur with high degree of probability. They were first observed at low energies [28]. An analogous result was obtained during the fragmentation of the neutron-deficient nucleus of ^{112}Sn. In the joint Dubna-GANIL experiments recently carried out in GANIL (France) the double-magic ^{100}Sn nucleus was produced [29]. At FLNR experiments are under way using reactions with ^{6}He nuclei produced in the ^{7}Li(40 MeV/A)+CH_2 reaction. With the aid of the transport system of the primary beam it has become possible to shape a ^{6}He beam with an energy resolution of 1%. The fragment-separator COMBAS project [30] is under way. Fragmentation reactions of the high-intensity primary beam of the U400M cyclotron will be used to produce beams of radioactive nuclei. The parameters of this separator are given in Table V. And finally, a storage ring project (the TREBLE Project) is under discussion [31]. Radioactive beams from the fragment-separator will be injected into it. Table VI presents the parameters of the radioactive beam storage ring. The storage ring will bring about a new and higher quality of radioactive beam research (monochromaticity, operation in continuous mode (high duty-factor value)). Multiple transitions of the nuclei through the target (10^6rev/s) will allow increasing the product yield of nuclear reactions with radioactive beams.

Table V.
Expected parameters of the COMBAS fragment-separation with other existing separators.

Comparison of Fragment Separators

Device	Ω (msr)	Δ p/p (%)	Max.(T·m)	Res.Power
LISE	1.0	5.0	3.2	800
FRS	0.7-2.5	2.0	9-18	240-1500
A1200	0.8-4.3	3.0	5.4	700-1500
RIPS	5.0	6.0	5.76	1500
COMBAS	6.4	20	4.5	4360

Table VI.
Basic parameters of the Ring K4

Ring	K4
$B\rho_{max}$, T•m	4
Circumference , m	83.11
Acceptance $\mathcal{E}$, π•mm•mrad	50
$(\Delta p/p)_{max}$, %	1.0
Cooling electron maximum energy , keV	100
Length of the cooling section , m	3
Electron maximum current , A	5
Cathode diameter , cm	3
RF amplitude, kV	14
Range of the RF frequency , MHz	0.5-3.4
Vacuum, Pa	10^{-8}

References

1. M.Brack et al., Rev. Mod. Phys. 44 (1972) 320.
2. Yu.Ts.Oganessian, in Classical and Quantum Mechanical Aspects in Heavy Ion Collisions, Lecture Notes in Physics, vol.33, Springer, Heidelberg, 1975.
3. W.J.Swiatecki, Nucl. Phys. A376 (82) 275.
   G.Munzenberg, Rep. Prog. Phys. 51 (1988) 57.
4. S.Hofmann, GSI Nachrichten, 01-90 (1990) 3.
5. Yu.A.Lazarev et al., in Proc. Int. School-Seminar on Heavy Ion Physics (Eds. Yu.Ts.Oganessian, Yu.E.Penionzhkevich, R.Kalpakchieva) Dubna 1993, vol.2, p.497.
6. A.V.Yeremin et al., Nucl. Instr. Meth. A274 (1989) 528.
7. Yu.A.Lazarev et al., Preprint E7-94-80, JINR Dubna 1994 (submitted to Phys. Rev. Lett.)
8. Z.Patyk et al., in Proc. Int. School-Seminar on Heavy Ion Physics, Dubna 1989, JINR Rept. D7-90-142, Dubna 1990, p.113.
9. Z.Patyk et al., Nucl. Phys. A533 (1991).
10. Yu.A.Lazarev et al., JINR FLNR Sci. Rep. 1991-1992, JINR Report E7-93-57, Dubna 1993, p.203.
11. H.C.Britt and A.R.Quinton, Phys. Rev. 124 (1961) 877.
12. C.Borcea et al., Nucl. Phys. A415 (1984) 169.
13. V.I.Zagrebaev, Ann. Phys. (N.Y.) 197 (1990) 33.
14. K.O.Oganessian et al., in Contributed Papers 5th Int. Conf. on Nucleus-Nucleus Collisions, Taormina, Italy 1994, p.65.
15. V.Zagrebarev, Yu.Penionzhkevich, Preprint GANIL P 93 20, 1993.

16. H.-G.Ortlepp et al., in Proc. Int. Conf. on Nucl. Physics with Advanced Techniques, Ierapetra, Greece 1991 (Eds. F.A.Beck etc., World Scientific) p.302.
17. M.K.Jones et al., Phys. Rev. C48 (1993) 2800.
18. I.Skwirczynska et al., Nucl. Phys A452 (1988) 432.
19. M.Colonna, M. Di Toro et al., Preprint LNS 03-03-94, Catania 1994.
20. V.V.Kamanin et al., Particles and Nuclei, vol. 20 (1989) p.741.
21. V.V.Kamanin et al., Z.Physk A327 (1987) 109.
22. P.Braun-Munzinger, J.Stachel, Ann. Rev. Nucl. Part. Sci. 37 (1987) 97.
23. A.A.Ogloblin, in Proc. Int. School-Seminar on Heavy Ion Physics (Eds. Yu.Ts.Oganessian, Yu.E.Penionzhkevich, R.Kalpakchieva) Dubna 1993, vol.1, p.28.
24. N.K.Skobelev et al., Z. Phys. A341 (1992) 315.
25. N.K.Skobelev et al., in Proc. Int. School-Seminar on Heavy Ion Physics (Eds. Yu.Ts.Oganessian, Yu.E.Penionzhkevich, R.Kalpakchieva) Dubna 1993, vol.1, p.51.
26. D.Guerreau, Conf. on HI Nuclear Collisions in the Fermi Energy Domain, Caen, France, 1986, J. de Physique C4-8, p.205.
27. A.C.Mueller et al., Nucl. Phys. A513 (1990) 1.
N.A.Orr et al., Preprint GANIL P 91 02 (1991).
M.Lewitowicz et al., Z.Physik A335 (1990) 117.
28. V.V.Volkov, Deep Inelastic Reactions, Energoizdat, Moscow, 1982.
29. M.Lewitowicz et al., JINR Rapid Communications N 6[63]-93.
30. A.G.Artukh et al., Nucl. Instr. Meth. A306 (1991) 123.
31. V.A.Gorshkov et al., in Proc. Int. School-Seminar on Heavy Ion Physics (Eds. Yu.Ts.Oganessian, Yu.E.Penionzhkevich, R.Kalpakchieva) Dubna 1993, vol.2, p.417.

Received by Publishing Department
on July 1, 1994.